Anal. Chem. **1997,** *69,* 3086−3094

The Electroactive Integrated Optical Waveguide: Ultrasensitive Spectroelectrochemistry of Submonolayer Adsorbates

Darren R. Dunphy,[†] Sergio B. Mendes,[‡] S. Scott Saavedra,*[,†] and Neal R. Armstrong*[,†]

Department of Chemistry and Optical Sciences Center, University of Arizona, Tucson, Arizona 85721

Highly sensitive spectroelectrochemistry of adsorbed films on ITO is demonstrated with the electroactive integrated optical waveguide (EA-IOW). The EA-IOW, a single-mode planar waveguide coated with an ITO layer, is ∼10^4-fold more sensitive to changes in absorbance occurring during electrochemical events versus a single-pass transmission spectroelectrochemical experiment, as demonstrated by reduction of surface-adsorbed methylene blue. Furthermore, the EA-IOW is selective to near-surface events, as it is relatively insensitive to absorbance by solutions of dissolved chromophores at < 1 mM. The EA-IOW is also used to monitor the formation of Prussian Blue during the reduction of ferricyanide, an event that is not easily followed using current-detected cyclic voltammetry, due to interfering faradaic and non-faradaic electrochemical events. The optical background of the EA-IOW is potential-dependent and is explained by ion diffusion into the ITO and by voltage-dependent changes in optical constants for the material. Finally, the high sensitivity of the EA-IOW (relative to other evanescent-field-based spectroelectrochemical techniques) is discussed in terms of its design.

Spectroelectrochemistry has proven useful in a number of electrochemical problems, including the study of redox mechanisms of simple probe molecules,[1,2] protein electrochemistry,[3] and redox processes of conducting polymers and molecular assemblies.[4] The primary advantage of spectroelectrochemical techniques is their ability to provide spectral data that are complementary to the current or voltage response of more conventional electroanalytical techniques.[1,2] As an example, absorbance measurements can be used to determine parameters such as diffusion coefficients or rate constants. These parameters may be difficult to determine with conventional electroanalytical measurements due to contributions from faradaic and non-faradaic background currents.[1,2]

Traditional spectroelectrochemical measurements that utilize a light path perpendicular to the electrode may lack sufficient sensitivity to probe redox processes occurring at or near the electrode surface due to the inherently small optical path length.[1,2] Using the evanescent field obtained from total internal reflection at an optically transparent electrode/solution interface, it is possible to selectively probe optical changes at the electrode/solution interface and increase sensitivity to these changes relative to that of a standard transmission experiment. Winograd and Kuwana, using a SnO_2/glass electrode in an ATR configuration with five reflections, were originally able to increase the absorbance sensitivity at an electrode/solution interface by a factor of ∼7 (compared to a single-pass transmission experiment).[5] More recently, Itoh and Fujishima increased the sensitivity of spectroelectrochemistry to changes in absorbance during a redox process by a factor of ∼150, utilizing a 2 μm thick, single-mode, gradient-index optical waveguide, overcoated with a thin tin oxide (SnO_2) film.[6,7] Other researchers have developed similar electrochemically active, multilayer waveguide devices for use as chemical sensor platforms, such as an optical, phthalocyanine-based chlorine sensor.[8,9] Surface plasmon resonance (SPR) techniques have also been applied to the characterization of environments at electrode surfaces.[10] SPR is sensitive to changes in *both* the real and imaginary portions of the refractive index at the electrode/electrolyte interface.[11,12] Under appropriate conditions, evanescent-field-based waveguide measurements are primarily sensitive to changes *only* in the imaginary portion of the refractive index.[13] However, it should be noted that the two techniques are complementary in terms of the electrode systems available for study (metals for SPR vs oxide surfaces for waveguides), and thus a direct comparison is not completely valid.

We report in this article a quantitative evaluation of a multilayer, single-mode waveguide electrode device, termed the electroactive integrated optic waveguide (EA-IOW). The EA-IOW in its present form is extremely sensitive to electrochemically driven absorbance changes in weakly absorbing films. It is estimated that the increase in sensitivity (relative to a single-pass transmission experiment) is on the order of ∼10^4. This is demonstrated

[†] Department of Chemistry.
[‡] Optical Sciences Center.

(1) Kuwana, T.; Winograd, N. In *Electroanalytical Chemistry*; Bard, A., Ed.; Marcel Dekker, Inc.: New York, 1974; Vol. 7, pp 1−78.
(2) Heineman, W. R.; Hawkridge, F. M.; Blount, H. N. In *Electroanalytical Chemistry*; Bard, A., Ed.; Marcel Dekker, Inc.: New York, 1984; Vol. 13, pp 1−113.
(3) Hawkridge, F. M.; Taniguchi, I. *Comments Inorg. Chem.* **1995**, *17*, 163−187.
(4) Ferencz, A.; Armstrong, N. R.; Wegner, G. *Macromolecules* **1994**, *27*, 1517−1526.
(5) Winograd, N.; Kuwana, T. *J. Electroanal. Chem.* **1969**, *23*, 333−342.
(6) Itoh, K.; Fujishima, A. *J. Phys. Chem.* **1988**, *92*, 7043−7045.
(7) Itoh, K.; Fujishima, A. In *Electrochemistry in Transition*; Murphy, O. J., Srinivasan, S., Conway, B. E., Eds.; Plenum Press: New York, 1992; pp 219−225.
(8) Piraud, C.; Mwarania, E.; Wylangowski, G.; Wilkinson, J.; O'Dwyer, K.; Schiffrin, D. J. *Anal. Chem.* **1992**, *64*, 651−655.
(9) Piraud, C.; Mwarania, E. K.; Yao, J.; Schiffrin, D. J.; Wilkinson, J. S. *J. Lightwave Technol.* **1992**, *10*, 693−699.
(10) Lavers, C. R.; Harris, R. D.; Hao, S.; Wilkinson, J. S.; O'Dwyer, K.; Brust, M.; Schiffrin, D. J. *J. Electroanal. Chem.* **1995**, *387*, 11−22
(11) Raether, H. In *Physics of Thin Films*; Haas, G., Francombe, M. H., Hoffman, R. W., Eds.; Academic Press: New York, 1977; Vol. 9, pp 145−261.
(12) Burstein, E.; Chen, W. P.; Hartstein, A. *J. Vac. Sci. Technol.* **1974**, *11*, 1004.
(13) Saavedra, S. S.; Reichert, W. M. *Anal. Chem.* **1990**, *62*, 2251−2256.

S0003-2700(96)01272-3 CCC: $14.00

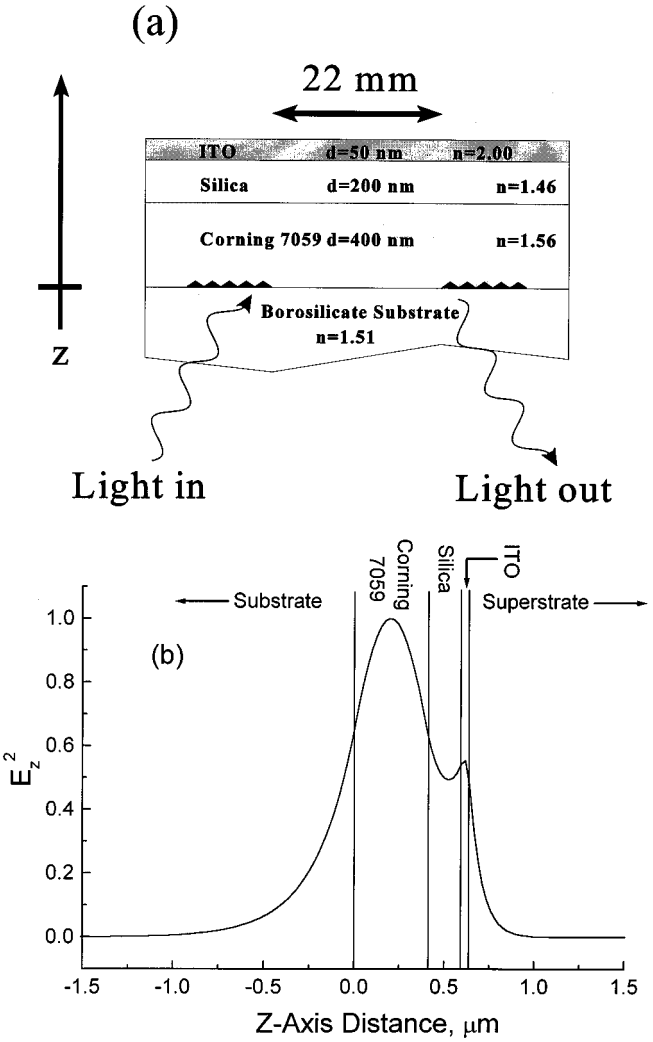

Figure 1. Diagrams of the EA-IOW. (a) Physical structure (not to scale) and (b) squared electric field amplitude (E_z^2) as a function of distance through the waveguide.

by measuring absorbance changes during the reduction of a low-surface-coverage film (< 0.4% of a full monolayer) of electrostatically adsorbed methylene blue. The expected sensitivity is also calculated theoretically and is found to agree with the experimental measurement within a factor of 4. Furthermore, measurements using a highly absorbing solution of a dye which interacts only weakly with the ITO surface show that optical changes detected with the EA-IOW are selective for surface-confined species, as expected.

Although at present the EA-IOW is capable of only spectrometric measurements at one wavelength in each experiment, the added dimensionality of the data obtained can be useful in the identification of products formed during electrochemical processes. As an example, EA-IOW data from the reduction of ferricyanide demonstrate the formation of an ultrathin film of Prussian Blue ($Fe_4(Fe(CN)_6)_3$), and its subsequent reduction to Prussian White (also called Everitt's salt, $K_2FeFe(CN)_6$), with a sensitivity which far surpasses that of the voltammetric data.

EXPERIMENTAL SECTION

Design and Construction of the EA-IOW. The EA-IOW, as diagramed in Figure 1a, is a multilayer structure consisting of Corning 7059 glass, silicon dioxide, and ITO deposited on a 7.5 cm × 2.5 cm × 1 mm soda lime glass substrate using a Perkin-Elmer 2400 rf diode sputtering system. The predeposition vacuum was 2×10^{-6} Torr: a reactive atmosphere of Ar (70%) and O_2 (30%) was dynamically controlled during the deposition by an MKS two-channel flowmeter to a constant pressure of 3.9×10^{-3} Torr. The previously calibrated deposition rates were 50, 62, and 133 Å/min for the 7059 glass, SiO_2, and ITO materials, respectively. The respective thicknesses of the three layers were 400, 200, and 50 nm. After ITO deposition, the EA-IOW was annealed for 1 h at 225 °C in air, yielding a measured resistivity of 1100 Ω/□. (Improved resistivity (under 800 Ω/□) in EA-IOWs has been achieved by using an improved annealing procedure that was implemented after the waveguide utilized in this report.) It is estimated that the propagation loss of the EA-IOW was ∼5 dB/cm (at 633 nm).

The input and output couplers were diffraction gratings fabricated by interfering two collimated beams in a Lloyd's mirror configuration.[14] The 441.65 nm output of the laser, a Kimmon He−Cd, was spatially filtered, expanded, and recollimated to 0.4 mW/cm^2. The substrate (spin-coated at 4000 rpm for 30 s to a thickness of ∼180 nm with Shipley 1805 photoresist diluted 1:1 with type P photoresist thinner) was exposed for 30 s. The gratings were then developed by immersion in a 20% (v/v) Shipley 351 developer solution in water for 90 s. The photoresist grating pattern was transferred to the soda lime glass substrate by a reactive ion milling process using freon gas in a home-built apparatus. The grating periods were determined to be ∼0.4 μm by measuring the diffraction angles in a Littrow configuration.[14] The distance between the two gratings was 22 mm.

Experimental Layout and Protocols. A 10 mW TEM_{00} 633 nm He−Ne laser (MWK, Inc.) served as the light source for all experiments. The beam was modulated at ∼1 kHz using an EG&G Model 192 chopper, and the outcoupled beam was detected with a biased photodiode (Newport Model 818-BB-21). The chopper reference and photodiode output were connected to an Ortec 9503 lock-in amplifier. The beam was focused onto the leading edge of the input grating of the EA-IOW with a 50 cm focal length lens through the waveguide substrate. The EA-IOW was mounted horizontally in a Lucite spectroelectrochemical flow cell, which was mounted on an XYZ positioning stage to adjust the incoupling location and a rotary stage to adjust the incoupling angle. This approach is similar to other configurations used for planar waveguide ATR experiments.[15] Both the incoupled and outcoupled beams were spatially filtered. Two separate experiments were performed to confirm that scattered light did not contribute significantly to light intensity measured at the photodiode. First, a small ink dot was placed on the waveguide surface to extinguish the mode propagating in the IOW: no measurable signal from the photodiode was observed. Second, a series of neutral density filters (from 10% to 85%) was placed between the waveguide output grating and the detector, and the percent transmission was measured relative to measurements made using a commercial UV/visible spectrometer (Hitachi U-2000). The values obtained for both systems were found to agree within a few percent, indicating that contributions from scattered light intensity were insignificant.

(14) Li, L.; Xu, M.; Stegeman, G. I.; Seaton, C. T. *Proc. SPIE-Int. Soc. Opt. Eng.* **1987**, *835*, 72−82.
(15) Yang, L.; Saavedra, S. S. *Anal. Chem.* **1995**, *67*, 1307−1314.

The Lucite flow cell exposed a 2.6 cm^2 area (0.6 cm wide) on the EA-IOW surface. The internal volume of the cell was approximately 2 mL. The EA-IOW was clamped to the cell using silicone sheeting as a gasket: a brass contact between the waveguide and gasket provided for an electrical connection to the ITO surface. The rear of the EA-IOW substrate was painted with a black strippable coating (Universal Photonics, Inc.) between the two gratings to prevent backscatter of light from the cell and to absorb any light scattered into the substrate modes. The cell also contained two ports opposite the EA-IOW for a counter electrode (platinum wire) and a reference electrode (a pseudo-Ag/AgCl electrode, which was periodically calibrated against the ferri-ferrocyanide redox couple to provide a potential scale properly referenced to the Ag/AgCl reference electrode). Solutions in the cell could be exchanged via external Luer fittings connected to the cell with Teflon tubing. The potential at the EA-IOW was controlled through a PAR Model 362 poteniostat, except during the measurement of methylene blue surface coverage, when a Cypress Systems CS-1090 was used.

Data collection and instrument control were achieved through the use of an AT-MIO-16XE-50 DAC board programmed using Labview software (both from National Instruments). An analog output channel was used to scan the potential through the external signal input of the PAR 362 at a rate of 10 mV/s (1 mV/potential step) for all experiments. Current, cell potential, and LIA output were clocked to be read after each analog output update. All data (except potential) were smoothed using a three-point moving boxcar average (which did not affect signal shape).

The EA-IOW was cleaned before each experiment by sonicating it first in HPLC-grade methylene chloride (Aldrich) for 15 min, followed by sonication in absolute ethanol for 15 min and a final sonication in Millipore water.

For all experiments, 0.1 M KCl in Millipore water was used as the supporting electrolyte. The EA-IOW was first cycled in electrolyte solution 10 times over the potential region of interest before each experiment. In addition, before the experiment involving methylene blue, the EA-IOW was allowed to sit in contact with the supporting electrolyte for 3 days in order to equilibrate the ITO with the electrolyte solution and to suppress any hysteresis in the optical background (vide infra).

Blue dextran (Sigma) solutions in water were prepared at concentrations of 2.0, 3.6, 5.7, and 6.8 μM. The blue dextran had an average molecular weight of 2×10^6 and a molar absorptivity of 1.8×10^6 M^{-1} cm^{-1} (at 633 nm). Between the measurements of each solution, the Lucite flow cell was flushed with Millipore water until the outcoupled light intensity returned to the value obtained before the introduction of blue dextran. For the spectroelectrochemical characterization of methylene blue (MB) reduction, four solutions of MB (Aldrich) were prepared in 0.1 M KCl at concentrations of 0.25, 0.5, 1.0, and 2.0 μM. Each solution was allowed to incubate in the cell for 10 min before the start of the experiment, and the cell was flushed with ~10 cell volumes of supporting electrolyte before introduction of the next MB solution. The concentration of the potassium ferricyanide solution used for the formation of Prussian Blue (PB) was 2 mM in 0.1 M KCl.

Theoretical Calculations. Theoretical calculations were carried out using Beta, a program written to numerically solve Maxwell's equations for multilayer waveguide structures.[16] The Corning 7059, SiO_2, ITO, and waveguide substrate were assumed to be nonabsorbing for all calculations (addition of a small absorptivity ($k = 0.01$) for the ITO did not alter the results of these calculations). For the simulation of waveguide sensitivity, the coefficient of the imaginary portion k of the refractive index for the absorbing film or sample solution was calculated from

$$k = \frac{\ln 10}{4\pi}\epsilon\lambda C \qquad (1)$$

where ϵ is the molar absorptivity of the absorbing species, C is the concentration, and λ is the wavelength.[17] Beta was used to calculate the effective refractive indexes (both real and imaginary) for the waveguide structure; the imaginary portion, N_I, was used to calculate absorbance using

$$\frac{I}{I_o} = \left|\frac{E}{E_o}\right|^2 = \exp\left(\frac{-4\pi N_I z}{\lambda}\right) \qquad (2)$$

where I and λ have their usual meanings, E is the amplitude of the electric field, and z is the distance between input and output grating couplers.[18]

For calculation of relative sensitivity compared to a transmission experiment, the absorbing molecules were assumed to be contained in a 20 Å thin film at the waveguide/superstrate interface, with a molar absorptivity of 10 000 $M^{-1}cm^{-1}$ and an assumed chromophore concentration of 1 mM. Variation of the absorbing layer thickness from 1 to 50 Å had little effect on the calculated absorbance (less than 1%).

RESULTS AND DISCUSSION

General Features of the EA-IOW. The use of optical waveguides for spectroscopic characterization of interfacial thin films has been extensively covered in various manuscripts and reviews.[19,20] A short description of the EA-IOW, however, will help clarify its operation. Figure 1a is a schematic of the EA-IOW, illustrating its structure. Corning 7059 is the principle waveguiding layer for the EA-IOW, as shown in Figure 1b, where the squared electric field amplitude calculated for the TE_0 mode of the EA-IOW is plotted as a function of distance across the device. The electric field amplitude is greatest in the 7059 glass layer, which is critical to operation of these devices, as too much power in the ITO layer will lead to unacceptable propagation loss in the EA-IOW. Indium tin oxide is a highly absorbing medium (when compared with waveguide materials such as 7059 glass); it also exhibits a large refractive index ($n = 2.0$) which shifts the electric field distribution into the ITO, further increasing optical losses due to absorbance. A significant benefit of this high refractive index, however, is an increase in waveguide sensitivity (vide infra). The thicknesses of the ITO layer (50 nm) and the silica layer (200 nm) were chosen as a compromise between optical loss in the waveguide, sensitivity, and electrode conductivity. The silica buffer layer present between the Corning 7059 and the ITO has two important functions. First, it is used to adjust the fraction of

(16) Li, L. *J. Opt. Soc. Am. A* **1994**, *11*, 984−991.
(17) Bard, A. J.; Faulkner, L. R. *Electrochemical Methods*; John Wiley & Sons: New York, 1980; p 586.
(18) Kogelnik, H. In *Theory of Optical Waveguides*; Tamir, T., Ed.; Springer-Verlag: New York, 1990; pp 12−53.
(19) Yang, L.; Saavedra, S. S.; Armstrong, N. R.; Hayes, J. *Anal. Chem.* **1994**, *66*, 1254−1263.
(20) Plowman, T.; Reichert, W. M.; Saavedra, S. S. *Biomaterials*, in press.

total power in the ITO layer. Second, it prevents ion diffusion from the Corning 7059 into the ITO during annealing.[21]

In Figure 1b, the evanescent field extends from the ITO surface into the superstrate; it probes both the superstrate and any adsorbed film on the waveguide surface. The exponential decay (calculated depth of penetration, ~100 nm) of the evanescent field provides the capability to perform spatially selective optical measurements of the environment adjacent to the waveguide surface.

Coupling of light into the EA-IOW is achieved through the use of grating couplers etched into the waveguide substrate.[14] Grating coupling is easier to implement experimentally than prism coupling, and once fabricated, the couplers are an integral, permanent part of the waveguide structure.[22]

Sensitivity of the EA-IOW. We assume a step function for the concentration−distance profile of absorbing molecules along the axis normal to the IOW surface. The total absorbance (A_{tot}) of light propagating in the IOW is

$$A_{tot} = A_f + A_b \tag{3}$$

where A_f denotes the absorbance contribution of the molecular film adsorbed to the waveguide surface, and A_b refers to the absorbance contribution of molecules in the bulk superstrate in contact with the adsorbed film. For weakly to moderately absorbing superstrates, the latter term may be ignored. This can be demonstrated by comparing the sensitivity of the EA-IOW to changes in superstrate absorbance with the sensitivity of a standard single-pass transmission experiment for the same solution. From Beer's law, the ratio of the sensitivities (equal to the ratio of absorbances) for the two different types of experiments can be related as

$$\frac{A_{IOW}}{A_{trans}} = \frac{b_{IOW}}{b_{trans}} \tag{4}$$

where the subscripts "IOW" and "trans" refer to the results from a waveguide and a transmission experiment, respectively. The term *b*, which has the usual meaning of cell path length for the transmission geometry, is defined in terms of *equivalent transmission cell path length* for the waveguide experiment. The equivalent transmission cell path length, which can be obtained from a plot of A_{IOW} vs A_{trans}, can be used to calculate A_b in eq 3.

Figure 2 contains the results of an experiment in which the absorbance of a series of solutions of blue dextran (a dye-labeled dextran) was measured using both the EA-IOW at open circuit and a cuvet with a path length of 1 mm in a standard transmission spectrometer. Blue dextran was chosen as the absorbing species as it is nonionic and thus is likely to interact only weakly with the waveguide surface (preventing significant contributions to A_{tot} from the first term in eq 3). At low concentrations of blue dextran (below ~4 μM), the plot of the EA-IOW absorbance in Figure 2 is linear (as theoretical calculations predict), but, at higher concentrations, the waveguide absorbance is greater than would be expected if the linear regime were to be extended. This nonlinearity is attributed to absorbance of light by surface-adsorbed blue dextran (A_f). To rule out the possibility of solution aggregation effects on dye molar absorptivity (which could arise due to the high solution concentration), the absorbance of each blue dextran solution diluted 1/50 was also measured in a 1 cm transmission cell. These data, multiplied by a factor of 5, are also plotted in Figure 2 and show that aggregation effects are not significant. Also plotted in Figure 2 is the theoretical waveguide absorbance calculated using Beta (assuming a molar absorptivity of 1.8×10^6 M^{-1} cm^{-1} for the blue dextran). The theoretical absorbance is greater at each concentration than the experimental data by a factor of 3−4, well within the errors typically found when making such calculations.[23−25] These data demonstrate that the expected absorbance vs concentration for the EA-IOW should be linear, even for such a highly absorbing superstrate. From the slope in the linear regime (0−4 μM), the experimental value of b_{IOW} is 0.14 mm (not atypical for single-mode IOW structures[13,26]). Given a path length of 0.14 mm, it is reasonable to expect that the term A_b in eq 3 may be ignored for all but very concentrated superstrates (i.e., solutions with $\epsilon C > \sim 10$). Thus, the EA-IOW will selectively probe optical absorbance changes in films of surface-confined molecules because the contribution of dissolved chromophores will be insignificant.

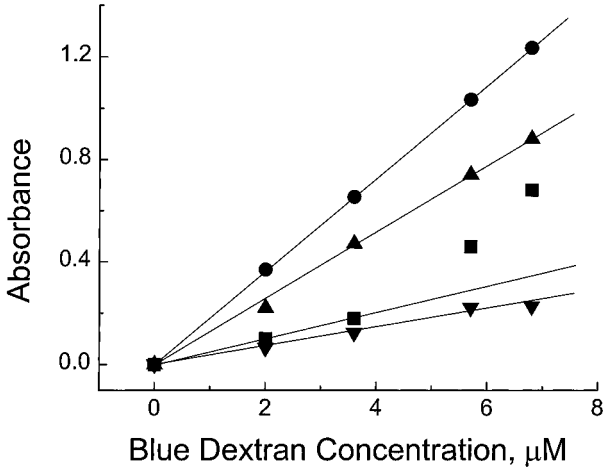

Figure 2. Absorbance of bulk dissolved blue dextran measured using ■, EA-IOW (multiplied by a factor of 2 for clarity); ●, a transmission geometry with a cuvet of 1 mm path length; ▼, a transmission geometry with a 1 cm path length cuvet, multiplied by 5, with each blue dextran solution diluted by a factor of 50; and ▲, theoretical EA-IOW absorbance.

Reduction of Surface-Adsorbed Methylene Blue. Methylene blue was chosen as the adsorbate to estimate the sensitivity of the EA-IOW to absorbance changes of surface-adsorbed species during electrochemical events for several reasons. First, MB is positively charged at pH 7 and is predicted to electrostatically adsorb to the negatively charged ITO surface. Also, MB is highly colored at 633 nm ($\epsilon = 7800$ M^{-1} cm^{-1}) and undergoes a reversible two-electron reduction to a colorless form at a potential of −0.275 V vs Ag/AgCl (as measured by the cyclic voltammetry of a 0.25 mM solution of MB in 0.1M KCl at an ITO electrode). Finally, at

(21) Davies, B. M.; Pannell, K. H. *J. Mater. Res.* **1994**, *9*, 226−228.
(22) Yang, L.; Saavedra, S. S.; Armstrong, N. R. *Anal. Chem.* **1996**, *68*, 1834−1841.
(23) Lee, J. E.; Saavedra, S. S., unpublished results.
(24) Plowman, T. E.; Garrison, M. D.; Walker, D. S.; Reichert, W. M. *Thin Solid Films* **1994**, *243*, 610−615.
(25) Walker, D. S.; Garrison, M. D.; Reichert, W. M. *J. Colloid Interface Sci.* **1993**, *157*, 41−49.
(26) DeGrandpre, M. D.; Burgess, L. W.; White, P. L.; Goldman, D. S. *Anal. Chem.* **1990**, *62*, 2012−2017.

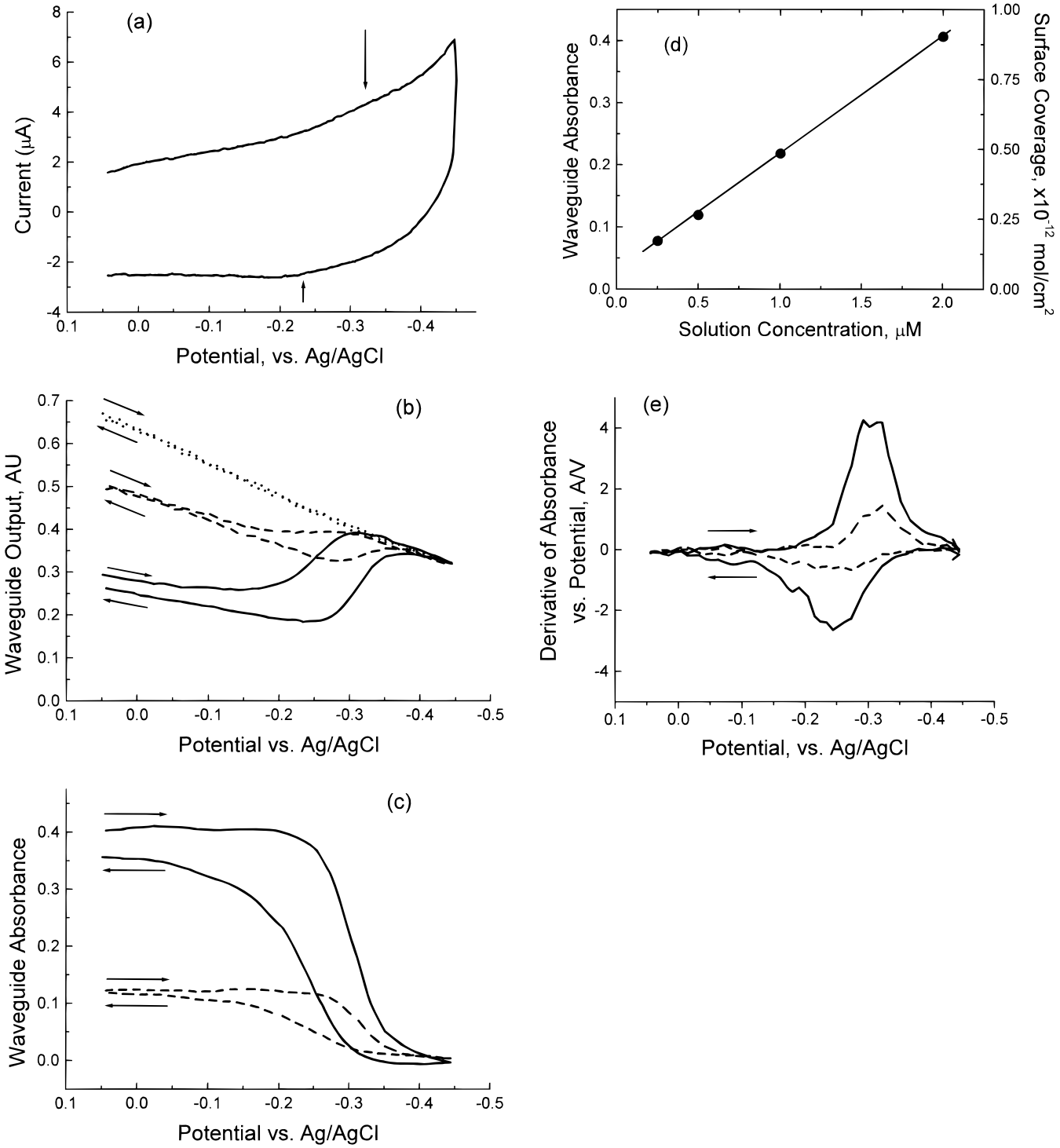

Figure 3. Reduction of methylene blue using the EA-IOW as the working electrode. (a) Conventional (current-detected) cyclic voltammogram of methylene blue, adsorbed from a 2.0 μM solution. The arrows indicate the signals for the reduction and oxidation process. (b) Optically detected cyclic voltammograms for the reduction of methylene blue. The arrows indicate scan direction. From top to bottom: dotted line, optical background (no methylene blue present); dashed line, 0.5 μM methylene blue signal; solid line, 2.0 μM methylene blue signal. (c) Absorbance vs potential calculated for the 0.5 μM (dotted line) and 2.0 μM (solid line) data in (b). (d) Methylene blue solution concentration vs waveguide absorbance and estimated surface coverage. (e) Reconstructed cyclic voltammograms using the data in (c).

the micromolar concentrations used for this study, the absorbance contribution from A_b (eq 3) is negligible. Thus, all changes in the optical signal will come solely from surface-confined MB.

Figure 3a is the cyclic voltammogram of a 2.0 μM MB solution using the EA-IOW as the working electrode with a scan rate of 50 mV/s. Because of the large non-faradaic charging current (due to a combination of space charge and solution double-layer capacitance[27]), the voltammetric signal is barely visible above the background and is even more difficult to distinguish at lower scan rates. However, after background subtraction, it is possible to measure voltammetric peak height and area to determine both surface coverage and the nature of the electrochemical process (diffusion-controlled or surface-confined). A plot of scan rate vs cathodic peak current for the 2.0 μM solution yielded a straight

(27) Armstrong, N. R.; Shepard, V. R. *J. Phys. Chem.* **1981**, *85*, 2965−2970.

line, indicating that the contribution to the total current from diffusion of MB to the EA-IOW can be ignored. From the slope of this line, the surface coverage Γ was calculated to be 9.0×10^{-13} mol/cm^2 for the 2.0 μM solution. This number agrees well with the surface coverage of 1.0×10^{-12} mol/cm^2 measured by integration of the cathodic peak in Figure 3a (after background subtraction). This number corresponds to less than ~0.4% of full monolayer coverage, based on a molecular area of 65 Å^2/molecule.[28]

The optical absorbance change associated with the reduction of the MB at the electrode surface, however, is measured easily using the EA-IOW, as shown in Figure 3b. The outcoupled light intensity increases dramatically (relative to the change observed in the absence of MB) during the scan from 50 to −450 mV (at 10 mV/s), corresponding to the reduction of surface-confined MB. Upon scan reversal, the surface-confined MB is reoxidized, and the waveguide output returns to almost the same level as that before the reduction scan. The signal is highly reproducible, as further scan cycles yield the same signal shape and magnitude. Furthermore, the optical responses obtained for all solution concentrations of MB measured in this series of experiments are identical in shape, differing only in magnitude of the maximal change in outcoupled light intensity (for clarity, only the signals for the 2.0 and 0.5 μM solutions are shown in Figure 3b).

By using the optical background signal change obtained in voltammetric experiments before the introduction of methylene blue as I_0 (the dotted line in Figure 3b), for this system it becomes possible to calculate an absorbance and determine *quantitative* spectrometric information, as demonstrated in Figure 3c for the reduction and reoxidation of both the 0.5 and 2.0 μM solutions. The absorbance changes measured are directly proportional to the solution concentration, as can be seen in Figure 3d. An equilibrium expression between adsorbed and dissolved MB can be written as

$$K_{ads} = \frac{\Gamma_{MB}}{[MB]} \tag{5}$$

where Γ_{MB} is the surface coverage of adsorbed MB (in mol/cm^2), [MB] is the superstrate MB concentration, and K_{ads} is the equilibrium constant. Since the surface coverage is directly proportional to the solution concentration, the absorbance measured by the EA-IOW is also directly proportional to surface coverage. Unfortunately, since the molar absorptivity of MB adsorbed to ITO is unknown, it is not possible to, a priori, calculate the surface coverage. Also, the equivalent transmission path length of the EA-IOW for surface-adsorbed molecules is not known. By using the electrochemically measured surface coverage of 1.0×10^{-12} mol/cm^2 for the 2.0 μM solution, however, it is possible to calculate the product of this sensitivity and MB molar absorptivity (analogous to ϵb in Beer's law) and use this product to calculate surface coverage for all other solution concentrations (right axis of Figure 3d). A value for the equilibrium constant K_{ads} of 4.2×10^{-4} cm can be calculated from Figure 3d.

The relative sensitivity of this electroactive waveguide compared with a transmission spectroelectrochemical reduction of MB was calculated to be over 40 000, which represents the ratio of effective path lengths, b_{IOW}/b_{trans}. Theoretical calculations estimate that the relative sensitivity should be ~12 000 for TE polarization (the theoretical relative sensitivity for the TM mode is only ~3500). It is not surprising that the experimental value is different from the theoretical value, as the effects of surface adsorption on the optical constants for MB are not known. It may not be possible to measure the relative sensitivity with a higher degree of certainty, as the optical constants for any molecular system do not necessarily scale with the increase in surface coverage needed to measure an absorbance in the transmission mode.

The measured absorbance vs potential is proportional to the integrated faradaic component of the cyclic voltammogram.[2] Starting with the equation for the $i-V$ curve of a surface-adsorbed electroactive species,[29] and assuming that the term A_b from eq 3 can be ignored, and that only one species (either the oxidized or reduced form of the surface adsorbate) absorbs light at the monitored wavelength, the derivative of the absorbance vs potential plot is given by

$$\frac{dA}{dE} = \frac{nF}{RT} \frac{\Gamma^* \epsilon S (b_o/b_r) \exp[(nF/RT)(E - E^{\circ\prime})]}{\{1 + (b_o/b_r) \exp[(nF/RT)(E - E^{\circ\prime})]\}^2} \tag{6}$$

where n, F, R, and T have their usual meanings, Γ^* is the total initial surface coverage of the adsorbate, ϵ is the molar absorptivity, $E^{\circ\prime}$ is the formal potential of the redox couple, E is the applied potential, and the ratio b_o/b_r is a measure of the relative strength of adsorption of the oxidized and reduced forms of the electroactive species. The term S is a sensitivity factor that depends on the strength of the evanescent field at the EA-IOW/solution interface, the thickness of the adsorbed layer, and the distance between input and output couplers. Thus, the derivative of Figure 3c, plotted in Figure 3e, is directly proportional to the faradaic current due to MB redox chemistry (by a factor $nFA\nu/\epsilon S$, where ν is the scan rate) *without contribution from non-faradaic background currents* (compare parts a and e of Figure 3). The shape of the cathodic signal is consistent with reduction of a surface-confined species. During the oxidation sweep, however, there is a negative displacement of the voltammetric peak and an increase in fwhm by a factor of 2. This effect could be due to either a diffusional process occurring after the desorption of the reduced form of methylene blue from the negatively charged ITO surface or the oxidation of a more energetically heterogeneous surface layer.

Formation of Prussian Blue. The added (spectrometric) dimension of the EA-IOW can be useful in the identification of new electrode processes. As an example, during the cyclic voltammetric reduction/oxidation of 2 mM $K_3(FeCN)_6$, using the EA-IOW as the working electrode, an additional electrochemical reduction was observed at 0.54 V, prior to the diffusion-controlled reduction of ferricyanide, which was accompanied by a change in the optical output of the EA-IOW. These changes were enhanced upon further voltammetric sweeps. The change in the optical signal was observed for the first sweep, but the voltammetric peak was not detected until it had grown sufficiently (in the third sweep) to be seen over the large background current of the ITO electrode. The voltammetric data from the third scan are presented in Figure 4a, and the optical data from the first and third scans are presented in parts b (optical signal) and c

(28) Adamson, A. W. *Physical Chemistry of Surfaces*; John Wiley & Sons, Inc.: New York, 1976; p 420.

(29) Reference 17, p 522.

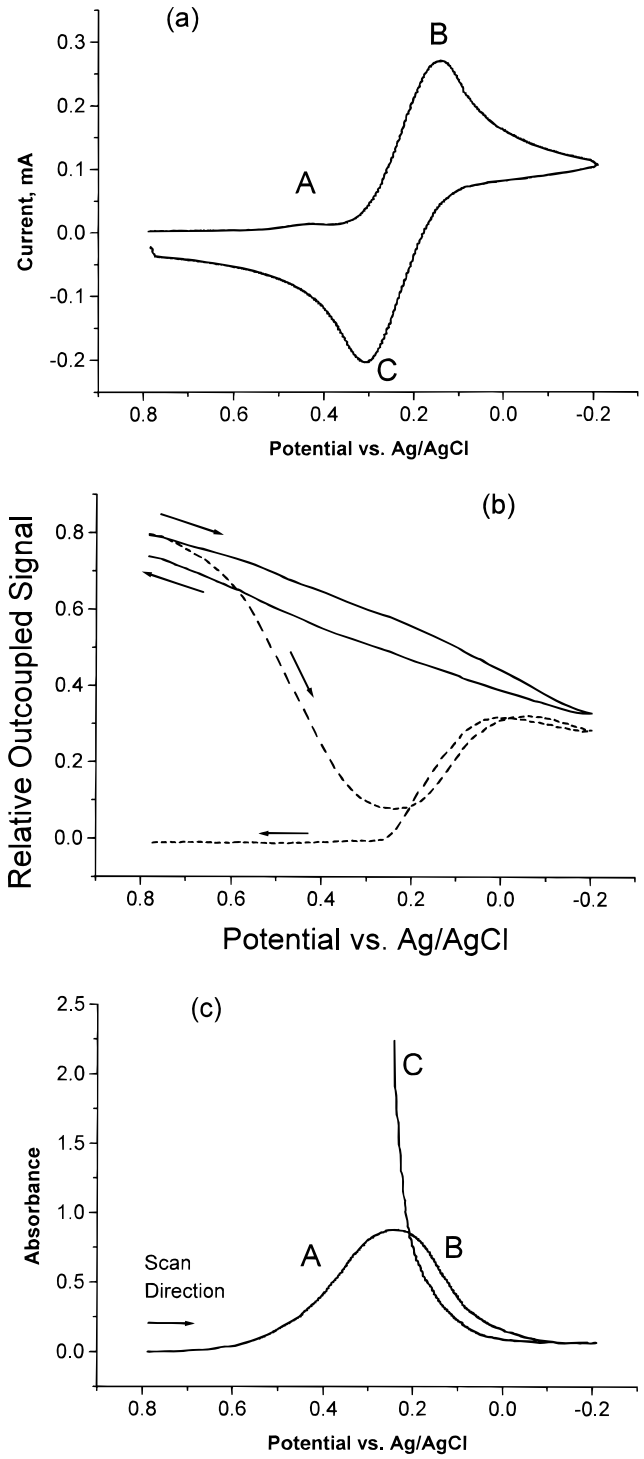

Figure 4. Formation of Prussian Blue during the reduction of ferricyanide at the EA-IOW surface. (a) Cyclic voltammogram for reduction of 2×10^{-3} M ferricyanide, third scan. Peaks B and C are due to the diffusion-controlled reduction and oxidation of the ferri-/ferrocyanide redox couple, while peak A is hypothesized to be due to the reduction of a Prussian Blue precursor. (b) Dashed line, optical data for scan 3; solid line, background before the introduction of ferricyanide. The arrows indicate scan direction. (c) Absorbance vs potential calculated from (b). Region A, formation of Prussian Blue; region B, reduction of Prussian Blue to Everitt's salt; region C, formation of more Prussian Blue.

(absorbance change calculated using the optical signal). The voltammetric data from the first and third scans are identical, except for the presence of the extra cathodic signal (at point A on Figure 4a) present only in the third scan. From the voltammetry alone, it is not possible to determine the origin of this extra cathodic peak. The scan dependence of this signal suggests that it is not due to a solution impurity but rather to the formation of a new surface-confined species. Based on the spectrometric information of the EA-IOW, it is hypothesized that the new species is, in fact, Prussian Blue (PB), most likely with the initial composition $Fe^{III}_4[Fe^{II}(CN)_6]_3$ (vide infra).[30−33]

The mechanism of PB formation at an electrode surface is not well understood.[32] The electrochemical synthesis of PB is normally accomplished by mixing equal amounts of $FeCl_3$ and $K_3Fe(CN)_6$ to form a precursor complex ($Fe^{III}-Fe^{III}(CN)_6$), which is then reduced to PB at a potential of ∼0.5 V vs SCE, the exact potential being dependent on solution composition and which iron in the complex is being reduced.[32] The onset of the increase in waveguide absorbance (Figure 4c) occurs in this potential range and is consistent with the electrochemical synthesis of PB (which is a strong absorber at 633 nm).[32] Furthermore, the EA-IOW absorbance subsequently decreases above 0.2 V, which is consistent with the reduction of PB to Everitt's salt, a colorless compound with the initial formula $K_4Fe^{II}_4[Fe^{II}(CN)_6]_3$.[31−33] It is possible that the precursor complex is formed in solution after the degradation of $Fe(CN)_6^{3-}$ to Fe^{III}, a process which may be facilitated in some manner by the surface of the ITO.

By integrating the current under the voltammetric peak at 0.54 V and assuming a 100% current efficiency for production of PB, it is possible to estimate a surface coverage of 2.7×10^{-10} mol/cm^2 for PB (equal to ∼1.7 equivalent monolayers using a square unit cell dimension of 10.16 Å).[34] This is clearly an overestimation, since the maximum absorbance is only 1.0, and subsequent EA-IOW experiments with monolayer coverages of other highly absorbing chromophores (e.g., phthalocyanines) have demonstrated that a single monolayer is too highly absorbing to perform spectroelectrochemistry using the EA-IOW.[35] Most likely, the current efficiency is much lower than 100%.

After the third scan, the film formed on the ITO surface was of sufficient thickness to quench all light in the EA-IOW and significantly alter the in- and outcoupling angles for the grating couplers, due to a large change in the effective refractive index of the guided mode. However, after the cell was flushed with 0.1 M KCl and the potential scanned several more times, the optical output returned to its baseline value.

Although it was possible to identify PB as the material deposited at the EA-IOW surface, the exact composition is unknown. Prussian Blue can take one of two formulations, the so-called "soluble" ($KFe^{III}[Fe^{II}(CN)_6]$) and "insoluble" ($Fe^{III}_4[Fe^{II}(CN)_6]_3$) forms.[30] An exact identification can be made by the observation of λ_{max} for the film (the maximum absorbance occurs at 730 nm for the insoluble form and 690 nm for the soluble material). It is believed that the insoluble form is the initial product of PB formation and that the soluble form is produced upon substitution of Fe^{III} by K^+ during voltammetric cycling. Because the EA-IOW is only capable of spectrometric measurements at present, classification of the PB's initial form is not

(30) Ellis, D.; Eckhoff, M.; Neff, V. D. *J. Phys. Chem.* **1981**, *85*, 1225−1231.
(31) Itaya, K.; Ataka, T.; Toshima, S. *J. Am. Chem. Soc.* **1982**, *104*, 4767−4772.
(32) Mortimer, R. J.; Rosseinsky, D. R. *J. Chem. Soc., Dalton Trans.* **1984**, 2059−2061.
(33) Garcia-Jareno, J. J.; Navarro-Laboulais, J.; Vicente, F. *Electrochim. Acta* **1996**, *41*, 835−841.
(34) Buser, H. J.; Schwarzenbach, D.; Petter, W.; Ludi, A. *Inorg. Chem.* **1977**, *16*, 2704−2710.
(35) Dunphy, D. R.; Armstrong, N. R.; Saavedra, S. S., unpublished results.

possible. In this regard, the utility of the EA-IOW technique would be significantly enhanced by the ability to measure broadband absorbance spectra,[36] which is an area under investigation.

Optical Baseline of the EA-IOW. An important comparison between the MB and PB data sets is the shape of the optical baseline signal. All baseline signals for the EA-IOW exhibit two components: a linear change with potential that is highly reproducible and a large hysteresis between the forward and reverse scans that decreases with increasing scan number. Both effects are likely caused by a change in optical constants in the ITO and/or the ITO/solution interface.[5,37] For the PB experiment, the EA-IOW was used immediately after cleaning and exhibits a large hysteresis between the forward and reverse voltammetric sweeps (the solid line in Figure 4b). In contrast, before the MB experiments, the EA-IOW was left to soak in 0.1 M KCl for ~3 days and has an optical baseline that lacks any of the hysteresis observed in the former data set (Figure 3b). It appears that this hysteresis in signal is due to a slow ion exchange occurring between the ITO and the electrolyte and that, by first equilibrating the ITO in electrolyte, this effect is minimized.[27] In separate experiments, we have seen that the magnitude of this hysteresis is dependent on solution composition, being larger for 0.1 M KBr than for 0.1 M KCl. Further experiments will better characterize this effect.

The source of the linear change in absorbance with potential has been attributed to a change in optical constants of the ITO as the potential is scanned.[5,37] This effect was characterized in the early ATR spectroelectrochemical studies conducted by Winograd and Kuwana.[5] Given a change in the electron concentration inside the ITO, the expected change in refractive index can be related as

$$\frac{\Delta n}{n} = {}^1/_2\left[\frac{\lambda^2}{\lambda^2 - \lambda_p{}^2}\right]\frac{\Delta N}{N} \qquad (7)$$

where N is the electron concentration per cubic centimeter, λ is the wavelength of observation, and λ_p is related to the plasma frequency of the semiconductor by $\omega_p = 2\pi/\lambda_p$. Changes in n could lead to the downward slope observed in the baseline if it was of sufficient magnitude to increase the fraction of light in the ITO layer. The change in n, however, is typically very small ($\sim 10^{-5}$)[5] and not large enough to shift the mode profile calculated in Figure 1b to any significant extent. Also, if the mode was being shifted toward the ITO/superstrate interface, an increase in EA-IOW sensitivity would be expected as the potential was scanned negative. This is not observed in Figure 3c; the absorbance of the adsorbed MB layer remains constant until MB undergoes reduction. Although there is an insufficient change in n to explain the baseline slope, changes in k (the coefficient of the imaginary component of the refractive index) also occur upon a change in potential. The absorbance of nearly transparent conductors such as ITO in the visible region can be attributed to free-carrier absorption by

$$A_{\text{freecarrier}} = \frac{\lambda^2 e^3 N t}{4\pi^2 \epsilon_0 c^3 n m^{*2} \mu} \qquad (8)$$

where e and c have their usual meanings as constants, t is the optical path length, ϵ_0 is the optical dielectric constant of the semiconductor material, m^* is the reduced mass of the electron, and μ is the carrier mobility.[37] As the change in A (and thus k) is directly proportional to N, this effect will dominate over the change in n (eq 7).

One final possible contribution to the optical baseline is the increase in refractive index at the electrode/bulk interface due to changes in composition of the electric double layer. To model this effect, the effect of placing a 10 Å thick adlayer at the ITO layer/electrolyte interface with a Δn of +0.05 greater than the bulk electrolyte was calculated.[5] Analogous to the increase in ITO refractive index (eq 7), no noticeable change in mode structure was observed, demonstrating that changes in double-layer optical constants may be ignored.

Comparison of the EA-IOW with Other Waveguide Geometries. The extraordinary sensitivity of the EA-IOW is a direct result of its structure, specifically its small thickness and high refractive index at the waveguide/superstrate interface. The sensitivity of a waveguide is a function of the total percentage of bound light present in the evanescent field. Using a ray optics model to describe light propagation,[13] this percentage is related to the number of reflections that occur per unit waveguide length. The earliest electroactive waveguides, multiple-internal reflection elements with comparatively large thicknesses (3 mm), supported about only one reflection per centimeter.[5] Decreasing waveguide thickness increases the number of reflections, and thus increases the interaction of the light in the waveguide with the superstrate above the electrode.[13] This increase in sensitivity was realized during the 1980s by decreasing the waveguide thickness into the micrometer range.[13] Itoh and Fujishima used an 8 μm thick, gradient-index, four-mode waveguide to increase sensitivity to optical changes during the reduction of MB by a factor of 20−40 relative to a transmission experiment.[6] Further enhancement in sensitivity was achieved by decreasing the waveguide thickness to 2 μm, creating a single-mode waveguide with a sensitivity increase over a transmission experiment of 150.[7]

The EA-IOW continues the trend of diminishing thickness by decreasing the waveguide dimensions into the submicrometer regime. As discussed above, the theoretical sensitivity increase for the EA-IOW is approximately 12 000. This dramatic sensitivity enhancement over other waveguide designs is due to several structural features. First, the EA-IOW is a step-index guide, making it inherently more sensitive than a gradient-index design.[38] Also, the total thickness of the EA-IOW is only 650 nm. At this dimension, 4.1% of the total light power in the waveguide is contained in the evanescent field (Figure 1). Increasing the Corning 7059 layer thickness by only 200 nm (making the total waveguide thickness 850 nm) would decrease this percentage theoretically by a factor of ~2, thus halving the absorbance sensitivity. Increasing the silica buffer layer by only 100 nm would have the same effect. The primary reason for the high sensitivity, however, is the presence of the ITO layer. A waveguide structure identical to the EA-IOW, but lacking the ITO, would contain only

(36) Mendes, S. B.; Li, L.; Burke, J. J.; Lee, J. E.; Dunphy, D. R.; Saavedra, S. S. *Langmuir* **1996**, *12*, 3374−3376.
(37) Chopra, K. L.; Major, S.; Pandya, D. K. *Thin Solid Films* **1983**, *102*, 1−46.
(38) Choquette, S. J.; Locasio-Brown, L.; Durst, R. A. *Anal. Chem.* **1992**, *64*, 55−60.

0.4% of its total power in the evanescent field. The ITO, because of its high refractive index, shifts the mode distribution toward the superstrate (see the "bump" in the field distribution that occurs in the ITO layer in Figure 1), increasing the field strength at the ITO/superstrate interface. Further sensitivity enhancement could be achieved easily by increasing the ITO layer thickness even a small amount; an increase of 10 nm would theoretically double the sensitivity. There is a practical limitation to increasing the ITO thickness, however, as losses in the waveguide need to be kept to a level where it is possible to measure the outcoupled light intensity after traversing a reasonable electrode area.

CONCLUSIONS

The EA-IOW has been shown to be a powerful device for the spectroelectrochemical characterization of ultrathin surface-adsorbed materials. Electrochemical events involving molecules at less than 1% of an equivalent monolayer are easily monitored, without interference from non-faradaic events. The information gained can be used to determine quantitative and qualitative characteristics of the adsorbed film. The utility of the EA-IOW approach could be significantly enhanced by developing a broadband coupling system for true multiwavelength EA-IOW measurements.[36]

ACKNOWLEDGMENT

This work was funded by grants to N.R.A. and S.S.S. from the National Science Foundation (Chemistry) and the Materials Characterization Program, State of Arizona. D.R.D. was supported by a Facility Sponsored Laboratory Fellowship from Associated Western Universities, Inc., under a grant from the U.S. Department of Energy through Battelle Pacific Northwest National Laboratories.

Received for review December 16, 1996. Accepted May 8, 1997.[⊗]

AC961272G

[⊗] Abstract published in *Advance ACS Abstracts,* June 15, 1997.